J|A|C|S ARTICLES

Published on Web 03/26/2010

Metal Sulfide in a C_{82} Fullerene Cage: A New Form of Endohedral Clusterfullerenes

Lothar Dunsch,*[,†] Shangfeng Yang,[†,‡] Lin Zhang,[†] Anna Svitova,[†] Steffen Oswald,[†] and Alexey A. Popov[†,§]

Department of Electrochemistry and Conducting Polymers and Institute of Complex Materials, Leibniz-Institute for Solid State and Materials Research, D-01171 Dresden, Germany, Hefei National Laboratory for Physical Sciences at Microscale & Department of Materials Science and Engineering, University of Science and Technology of China (USTC), Hefei 230026, China, and Department of Chemistry, Moscow State University, Moscow 119992, Russia

Received November 11, 2009; E-mail: l.dunsch@ifw-dresden.de

Abstract: The row of endohedral fullerenes is extended by a new type of sulfur-containing clusterfullerenes: the metal sulfide (M_2S) has been stabilized within a fullerene cage for the first time. The new sulfur-containing clusterfullerenes $M_2S@C_{82}$-C_{3v}(8) have been isolated for a variety of metals (M = Sc, Y, Dy, and Lu). The UV−vis−NIR, electrochemical, and FTIR spectroscopic characterization and extended DFT calculations point to a close similarity of the $M_2S@C_{82}$ cage isomeric and electronic structure to that of the carbide clusterfullerenes $M_2C_2@C_{2n}$. The bonding in $M_2S@C_{82}$ is studied in detail by molecular orbital analysis as well as with the use of quantum theory of atom-in-molecules (QTAIM) and electron localization function (ELF) approaches. The metal sulfide cluster formally transfers four electrons to the carbon cage, and metal−sulfur and metal−carbon cage bonds with a high degree of covalency are formed. Molecular dynamics simulations show that Sc_2S cluster exhibits an almost free rotation around the C_3 axis of the carbon cage, resulting thus in a single line ^{45}Sc NMR spectrum.

Introduction

The world of endohedral fullerenes[1−7] comprises a large variety of structures encaged in different sizes and symmetries of carbon cages. Conventional endohedral metallofullerenes such as $La@C_{82}$ are distinguished by encapsulation of metal ions in the carbon cage to give a charge distribution like $La^{3+}@C_{82}^{3-}$. Besides these monometallic fullerenes that have been isolated as the first endohedral structures,[1] there also exists a larger number of di- and trimetallic structures in fullerene cages.[1,8] In most cases, the high content of metal ions in an endohedral fullerene can only be achieved by a cluster formation with nonmetals (such as nitrogen in $M_3N@C_{2n}$,[4,9−16] carbide unit in $M_{2,3,4}C_2@C_{2n}$,[17−23] CH group in $Sc_3CH@C_{80}$,[24] or oxygen in $Sc_4O_{2,3}@C_{80}$[25]), the resulting endohedral fullerenes being called "clusterfullerenes. Given that the types of "clusterfullerenes" reported so far are quite limited (only four as mentioned above), whereas the formation of clusterfullerenes and particularly of the metal nitride clusterfullerenes, has been demonstrated to be a practical way to enlarge the members of the clusterfullerene family and/or promote its production yield,[7,12,13] an intriguing question is whether clusters other than the aforementioned four types could be encapsulated into the fullerene cage.

† Leibniz-Institute for Solid State and Materials Research Dresden.
‡ University of Science and Technology of China.
§ Moscow State University.

(1) Shinohara, H. *Rep. Prog. Phys.* **2000**, *63* (6), 843–892.
(2) Akasaka, T.; Nagase, H. *Endofullerenes: A New Family of Carbon Clusters*; Kluwer: Dordrecht, 2002.
(3) Dunsch, L.; Yang, S. F. *Phys. Chem. Chem. Phys.* **2007**, *9* (24), 3067–3081.
(4) Dunsch, L.; Yang, S. *Small* **2007**, *3* (8), 1298–1320.
(5) Dunsch, L.; Yang, S. *Electrochem. Soc. Interface* **2006**, *15* (2), 34–39.
(6) Popov, A. A. *J. Comput. Theor. Nanosci.* **2009**, *6* (2), 292–317.
(7) Chaur, M. N.; Melin, F.; Ortiz, A. L.; Echegoyen, L. *Angew. Chem., Int. Ed.* **2009**, *48*, 7514–7538.
(8) Popov, A. A.; Zhang, L.; Dunsch, L. *ACS Nano* **2010**, *4* (2), 795–802.
(9) Stevenson, S.; Rice, G.; Glass, T.; Harich, K.; Cromer, F.; Jordan, M. R.; Craft, J.; Hadju, E.; Bible, R.; Olmstead, M. M.; Maitra, K.; Fisher, A. J.; Balch, A. L.; Dorn, H. C. *Nature* **1999**, *401* (6748), 55–57.
(10) Stevenson, S.; Fowler, P. W.; Heine, T.; Duchamp, J. C.; Rice, G.; Glass, T.; Harich, K.; Hajdu, E.; Bible, R.; Dorn, H. C. *Nature* **2000**, *408* (6811), 427–428.
(11) Dunsch, L.; Krause, M.; Noack, J.; Georgi, P. *J. Phys. Chem. Solids* **2004**, *65* (2−3), 309–315.
(12) Krause, M.; Wong, J.; Dunsch, L. *Chem.—Eur. J.* **2005**, *11* (2), 706–711.
(13) Yang, S. F.; Dunsch, L. *J. Phys. Chem. B* **2005**, *109* (25), 12320–12328.
(14) Chaur, M. N.; Melin, F.; Elliott, B.; Athans, A. J.; Walker, K.; Holloway, B. C.; Echegoyen, L. *J. Am. Chem. Soc.* **2007**, *129* (47), 14826–14829.
(15) Melin, F.; Chaur, M. N.; Engmann, S.; Elliott, B.; Kumbhar, A.; Athans, A. J.; Echegoyen, L. *Angew. Chem., Int. Ed.* **2007**, *46* (47), 9032–9035.
(16) Chaur, M. N.; Melin, F.; Ashby, J.; Kumbhar, A.; Rao, A. M.; Echegoyen, L. *Chem.—Eur. J.* **2008**, *14* (27), 8213–8219.
(17) Wang, C. R.; Kai, T.; Tomiyama, T.; Yoshida, T.; Kobayashi, Y.; Nishibori, E.; Takata, M.; Sakata, M.; Shinohara, H. *Angew. Chem., Int. Ed.* **2001**, *40* (2), 397–399.
(18) Shi, Z. Q.; Wu, X.; Wang, C. R.; Lu, X.; Shinohara, H. *Angew. Chem., Int. Ed.* **2006**, *45* (13), 2107–2111.
(19) Iiduka, Y.; Wakahara, T.; Nakajima, K.; Tsuchiya, T.; Nakahodo, T.; Maeda, Y.; Akasaka, T.; Mizorogi, N.; Nagase, S. *Chem. Commun.* **2006**, (19), 2057–2059.

The serious drawback of the standard arc-discharge synthesis of endohedral fullerenes is the preferable formation of the empty fullerenes, the metallofullerenes being only a fraction with few percent yields.[1] To solve this problem we have proposed a new route (the "reactive gas atmosphere" method) for metal nitride clusterfullerene production.[11,26] In this method, the nonmetal forming the central cluster atom is present in a larger concentration in the plasma (e.g., in the form of NH_3, if nitride clusterfullerenes are the main target of synthesis). In general the addition of a nonmetal to the arc-burning chamber for the cluster formation is to be managed in such a way that this nonmetal does not block the fullerene formation in total but affords a sufficient amount of the new endohedral cluster. In this work we followed such a concept to use a solid source containing the nonmetal sulfur to form a new sulfide clusterfullerene structure: $M_2S@C_{82}$ (M = Sc, Y, Dy, and Lu). As sulfur (like oxygen) is expected to suppress the fullerene formation, its effective concentration in the arc-discharge reactor was to be reduced by using a small amount of the nonmetal source. In this way, the new sulfide clusterfullerenes $M_2S@C_{82}$ embrace an encaged bimetallic sulfide cluster, $M_2^{III}S$, which is not stable in such a composition without the fullerene cage. The isolated $M_2S@C_{82}$ was characterized by MS, UV−vis−NIR, FTIR, and ^{45}Sc NMR and computed by DFT with the aim to determine its cage isomeric structure as well as the electronic structure and the dynamics of the sulfide cluster. Since the inclusion of metal nitride clusters (Gd_3N) in the C_{82} cage results in the formation of non-IPR structures,[27] whereas the IPR structures of C_{82} are the most abundant cage for the monometallofullerens, we also address the IPR nature of $M_2S@C_{82}$ synthesized in this work, and thus both the endohedral structure and the cage symmetry are of high interest for the field of endohedral fullerenes.

Results and Discussion

Synthesis of $Sc_2S@C_{82}$. For sulfur as a Group VI element, its presence could result in low weight compounds based on CS_2 without any fullerene cage formation. As a result, our earlier attempts using elemental sulfur and a metal (like yttrium) did not result in the reasonable formation of sulfide endohedral fullerenes, and therefore we preferred to have an additional element available that is well-known to form endohedral fullerenes. Furthermore the presence of oxygen as in many gaseous compounds of sulfur is to be avoided as this would interfere with the formation of sulfide structure formation as well. Hence we managed to introduce nitrogen in the solid source, and the choice of such a source was guanidium thiocyanate ($CH_5N_3 \cdot HSCN$, in abbreviation GT), which was added to the metal/graphite powder mixture. The production of the sulfide cluster fullerenes was fulfilled by the modified Krätschmer−Huffman method using the GT/metal/graphite powder mixture in an optimized molar ratio of GT/metal/C = 2.5:1:10, metal M = Sc, Y, Dy, and Lu (see Supporting Information S1 for the determination of the optimized conditions for the synthesis of $Dy_2S@C_{82}$). During the arc burning process the increase of the pressure of the atmosphere in the chamber points to the formation of further gaseous products from the graphite mixture. In this way the situation is somewhat comparable to that of the "reactive gas atmosphere" method.[3,11]

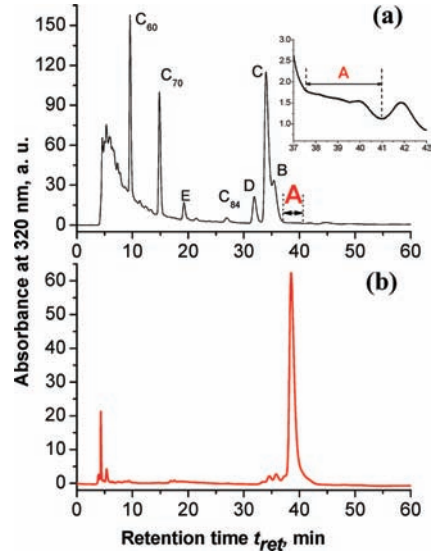

Figure 1. (a) HPLC chromatogram of the GT/Sc/C extract containing $Sc_2S@C_{82}$. **B**: $Sc_3N@C_{80}$ (II). **C**: $Sc_3N@C_{80}$ (I). **D**: $Sc_3N@C_{78}$. **E**: $Sc_3N@C_{68}$. Inset: enlarged chromatographic region of 37−43 min containing fraction A. (b) HPLC chromatogram of the isolated $Sc_2S@C_{82}$. HPLC conditions for (a) and (b): linear combination of two 4.6 mm × 250 mm Buckyprep columns; flow rate 1.6 mL/min; injection volume 100 μL; toluene as eluent (mobile phase); 40 °C.

The soot produced with the above given composition of the graphite rods was extracted by CS_2 for 20 h and analyzed by high performance liquid chromatography (HPLC) and laser desorption time-of-flight mass spectrometer (LD-TOF-MS). Figure 1a shows the HPLC profile of the extract obtained from the GT/Sc/C mixture by taking Sc as an example. The LD-TOF-MS analysis of the GT/Sc/C extract in comparison with that of the Sc/C extract without addition of GT indicates a new mass peak at 1106. Therefore fractions with t_{ret} of 18.5−40.5 min (fractions **A**−**E** and C_{84}), which are well-known based on the Sc/C extract, were isolated and subjected to further LD-TOF-MS analysis, revealing that the new mass peak at 1106 exists only in fraction **A** (t_{ret} = 37.5−40.9 min, see inset of Figure 1a).

Fraction **A** was further separated by recycling HPLC running in a Buckyprep-M column, resulting in the isolation of two fractions (**A-1** and **A-2**, see Supporting Information S4). The LD-TOF-MS examination of fraction **A-1** reveals a single MS peak at 1106 (see Figure 2), indicating the successful isolation of the new compound after removal of the fraction **A-2**. The purity of the isolated new compound was further checked by HPLC as illustrated in Figure 1b, suggesting a purity of ca.

(20) Iiduka, Y.; Wakahara, T.; Nakahodo, T.; Tsuchiya, T.; Sakuraba, A.; Maeda, Y.; Akasaka, T.; Yoza, K.; Horn, E.; Kato, T.; Liu, M. T. H.; Mizorogi, N.; Kobayashi, K.; Nagase, S. *J. Am. Chem. Soc.* **2005**, *127* (36), 12500–12501.
(21) Yang, H.; Lu, C.; Liu, Z.; Jin, H.; Che, Y.; Olmstead, M. M.; Balch, A. L. *J. Am. Chem. Soc.* **2008**, *130* (51), 17296–17300.
(22) Inoue, T.; Tomiyama, T.; Sugai, T.; Okazaki, T.; Suematsu, T.; Fujii, N.; Utsumi, H.; Nojima, K.; Shinohara, H. *J. Phys. Chem. B* **2004**, *108* (23), 7573–7579.
(23) Wang, T.-S.; Chen, N.; Xiang, J.-F.; Li, B.; Wu, J.-Y.; Xu, W.; Jiang, L.; Tan, K.; Shu, C.-Y.; Lu, X.; Wang, C.-R. *J. Am. Chem. Soc.* **2009**, *131* (46), 16646–16647.
(24) Krause, M.; Ziegs, F.; Popov, A. A.; Dunsch, L. *ChemPhysChem* **2007**, *8* (4), 537–540.
(25) Stevenson, S.; Mackey, M. A.; Stuart, M. A.; Phillips, J. P.; Easterling, M. L.; Chancellor, C. J.; Olmstead, M. M.; Balch, A. L. *J. Am. Chem. Soc.* **2008**, *130* (36), 11844–11845.
(26) Dunsch, L.; Bartl, A.; Georgi, P.; Kuran, P. *Synth. Met.* **2001**, *121* (1−3), 1113–1114.
(27) Mercado, B. Q.; Beavers, C. M.; Olmstead, M. M.; Chaur, M. N.; Walker, K.; Holloway, B. C.; Echegoyen, L.; Balch, A. L. *J. Am. Chem. Soc.* **2008**, *130* (25), 7854–7855.

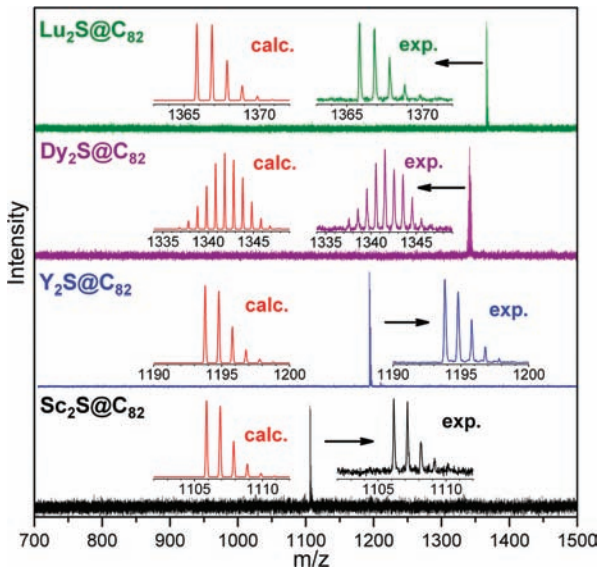

Figure 2. LD-TOF-MS of $Sc_2S@C_{82}$, $Y_2S@C_{82}$, $Dy_2S@C_{82}$, and $Lu_2S@C_{82}$ (positive-ion mode; analogous spectra were also measured in the negative-ion mode). The insets show experimental and calculated isotopic distribution for the corresponding $M_2S@C_{82}$ species.

92%, which is essentially high for the following spectroscopic characterizations.

As the MS peak of 1106 was detected only in the GT/Sc/C extract and was not available in the Sc/C extract or the empty fullerene extract, the new compound with the mass number of 1106 should contain sulfur. The presence of sulfur was confirmed by XPS study of fraction **A** (see Supporting Information S3). Accordingly, searching all of the possible formulations derived from the mass number of 1106 with sulfur and scandium, only 4 structures among the 7 possible formulations[28] have an even number of carbon atoms, i.e., $(Sc_2S)C_{82}$, $(Sc_2S_4)C_{74}$, $(Sc_2S_3N_4)C_{72}$, and $(Sc_4S_3N)C_{68}$. Since the new compound of 1106 *m/z* was isolated from fraction **A** for which the retention time on the Buckyprep column is even longer than that of $Sc_3N@C_{80}$ (fractions **B** and **C**), the carbon cage of the new compound (fraction **A-1**) should be comparable to or larger than C_{80} according to the elution behavior of the Buckyprep column. Therefore, the latter three formulations with much smaller carbon cages are excluded, and only the first formulation with an endohedral structure, $Sc_2S@C_{82}$, can be assigned to the new MS peak at 1106. The isotopic distribution of this MS peak at 1106 shows a good agreement with the calculated one of $Sc_2S@C_{82}$ (see Figure 2), confirming the proposed chemical formulation. Furthermore, the other 3 formulations require that the larger clusters (with more than six atoms, as denoted by the species in the parentheses) are encapsulated within the smaller carbon cages, which is hardly possible because of the size limitations. An alternative structure of $Sc_2O_2C_{82}$ with the same mass number of 1106 can be excluded on the basis of the exclusive formation of the new compound only by using GT in the raw material, which is essential as the sulfur source (see Supporting Information S2). Besides, the presence of oxygen in the arc-discharge plasma results in the first head in the formation of $Sc_4O_{2,3}@C_{80}$ clusterfullerenes,[25,29] none of which has been observed in our work.

The definitive proof of the $M_2S@C_{82}$ formulation for the new clusterfullerene type is obtained from the studies of the other metals. In addition to the $Sc_2S@C_{82}$, our new synthetic route to the metal sulfide clusterfullerenes was also probed for several other Group III metals including yttrium, dysprosium, and lutetium. In the GT/metal/graphite arc-discharge burnings, all of these metals afforded formation of the similar new species, whose mass spectra are consistent with the $M_2S@C_{82}$ (M = Y, Dy, Lu) formulations (see Figure 2). Thus, we have shown that a brand-new type of endohedral clusterfullerenes, sulfide clusterfullerenes, can be routinely prepared for a variety of representative metals with different ionic radii (from the relatively small Sc through intermediate size Lu to the larger Dy and Y) and propensity for endohedral fullerene formation.

Interestingly, during our study we noticed that the corresponding nitride clusterfullerenes formed simultaneously along with the sulfide clusterfullerene, and the yield of nitride clusterfullerenes was even comparable to that by using the reactive gas atmosphere method. Therefore, it is instructive to compare the yield of $Sc_2S@C_{82}$ to that of $Sc_3N@C_{80}$ (I). The relative yield of $Sc_2S@C_{82}$ to $Sc_3N@C_{80}$ (I) has been estimated to be 1:150 on the basis of the integrated area of the corresponding peaks in the chromatogram (see Supporting Information S5). Using a 2 g mixture of GT/Sc/C, 15−20 mg of $Sc_3N@C_{80}$ (I) and ca. 0.1 mg of purified $Sc_2S@C_{82}$ can be collected by our method. The high yield of C_{80}-I_h(7) based clusterfullerenes with the formal 6-fold electron transfer to the carbon cage as compared to all other carbon cages with the same endohedral cluster has been explained by an exclusive stability of the C_{80}^{6-}-I_h(7) hexaanion.[30] When the formation of this cage is not favored (for instance, when the number of the transferred electrons is different from six), much lower yields of endohedral fullerenes are observed for this cage size. The absence of the C_{80}-I_h(7) cage encapsulating the Sc_2S cluster suggests that the number of the electrons transferred to the carbon cage is decisive.

Spectroscopic Characterization. Among the isolated sulfide clusterfullerenes $M_2S@C_{82}$ we focus on the characterization of $Sc_2S@C_{82}$ as Sc-based endohedral fullerenes are usually synthesized with higher yield. Figure 3 compares the UV−vis−NIR absorption spectra of three sulfide clusterfullerenes including $Sc_2S@C_{82}$, $Dy_2S@C_{82}$, and $Lu_2S@C_{82}$ to a set of other endohedral metallofullerenes with a C_{82} carbon cage, including $Sc_2C_2@C_{82}$-C_{3v}(8), $Sc@C_{82}$-C_{2v}(9), and $Dy_3N@C_{82}$-C_s(39663). The conservative estimation of the optical band gap of $Sc_2S@C_{82}$ from the spectral onset (ca. 1240 nm) shows that it exceeds 1.0 eV. Therefore sulfide clusterfullerenes can be classified as kinetically stable fullerenes. Since absorption spectra of empty fullerenes as well as endohedral fullerenes in the visible and NIR ranges are dominated by the $\pi-\pi^*$ excitations of the carbon cage, the spectra are very sensitive to carbon cage isomerism and, on the other hand, are relatively insensitive to the nature of the encapsulated species. With this respect, comparison of the absorption spectrum of $Sc_2S@C_{82}$ to the spectra of C_{82}-based endohedral fullerenes with known cage isomers can support the structure elucidation of $Sc_2S@C_{82}$. Figure 3 clearly shows that the spectrum of the sulfide clusterfullerene $Sc_2S@C_{82}$ closely resembles that of the carbide clusterfullerene with C_{3v}(8) cage isomers both in terms of the band gap and peak positions (the spectra of $Sc_2C_2@C_{82}$ with

(28) That is, $(Sc_2S)C_{82}$, $(Sc_2S_2N_2)C_{77}$, $(Sc_2S_4)C_{74}$, $(Sc_2S_3N_4)C_{72}$, $(Sc_4SN_3)C_{71}$, $(Sc_4S_3N)C_{68}$, $(Sc_4S_4N_3)C_{63}$.

(29) Mercado, B. Q.; Olmstead, M. M.; Beavers, C. M.; Easterling, M. L.; Stevenson, S.; Mackey, M. A.; Coumbe, C. E.; Phillips, J. D.; Phillips, J. P.; Poblet, J. M.; Balch, A. L. *Chem. Commun.* **2010**, *46*, 279–281.
(30) Popov, A. A.; Dunsch, L. *J. Am. Chem. Soc.* **2007**, *129* (38), 11835–11849.

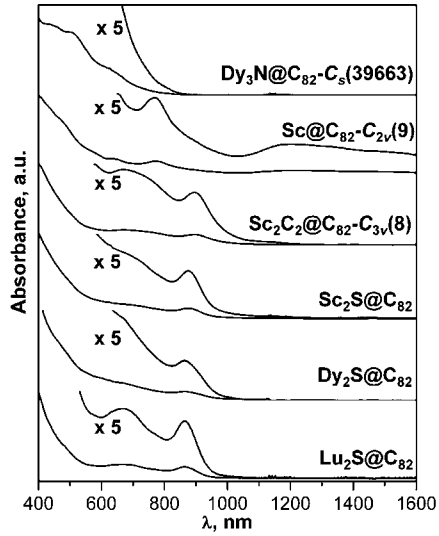

Figure 3. UV−vis−NIR spectra of $Sc_2S@C_{82}$, $Dy_2S@C_{82}$, and $Lu_2S@C_{82}$ in comparison to those of other endohedral fullerenes with C_{82} carbon cage, including $Sc_2C_2@C_{82}$-C_{3v}(8),[31] $Sc@C_{82}$-C_{2v}(9),[32] and $Dy_3N@C_{82}$-C_s(39663).[13]

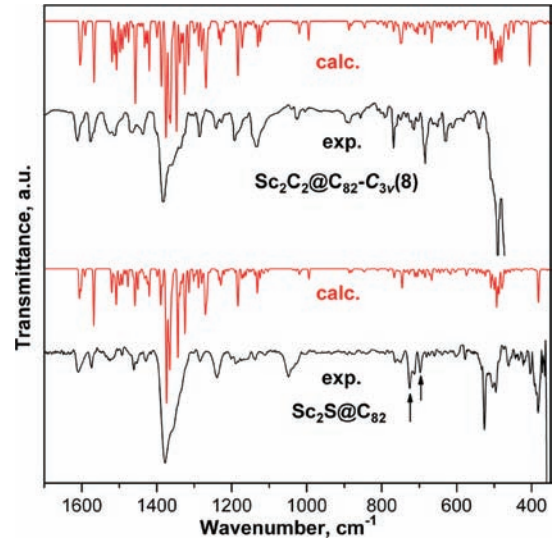

Figure 4. FTIR spectra of $Sc_2S@C_{82}$ and $Sc_2C_2@C_{82}$-C_{3v}(8) (from ref 34) in comparison to the corresponding DFT-simulated spectra. Arrows denote the solvent (toluene) lines.

other cage isomer are also available[31] but are substantially different from the spectrum of $M_2S@C_{82}$). On the other hand, $Sc@C_{82}$-C_{2v}(9)[32] has a much smaller HOMO−LUMO gap and hence its spectrum is extended to the NIR range, while $Dy_3N@C_{82}$-C_s(39663) has a larger band gap and its spectrum[13] exhibits substantially different features in the 400−800 nm range. Thus, from the results of UV−vis−NIR spectroscopic study we conclude that the electronic state of the carbon cage in $Sc_2S@C_{82}$ is the same as in the carbide clusterfullerene and that the most probable cage isomer of $Sc_2S@C_{82}$ is the same as that of $Sc_2C_2@C_{82}$-C_{3v}(8). Furthermore, the absorption spectra of $Dy_2S@C_{82}$ and $Lu_2S@C_{82}$ are also very similar to the spectrum of $Sc_2S@C_{82}$ (see Figure 3), which is a clear indication of the same fullerene cage in the three isolated sulfide clusterfullerenes.

Cyclic voltammetry study (*o*-DCB solution, $TBABF_4$ as supporting electrolyte) has shown that at the scan rate of 0.05 $V \cdot s^{-1}$ $Sc_2S@C_{82}$ exhibits one irreversible reduction at a peak potential of −1.03 V vs $Fc^{+/0}$ and a corresponding reoxidation peak at −0.51 V (at the scan rate of 1.0 $V \cdot s^{-1}$ the peak potentials are shifted to −1.07 and −0.45 V, respectively) followed by two reversible steps at −1.16 and −1.61 V. In the anodic range, one reversible oxidation step at 0.48 V was observed. The redox properties of $Sc_2S@C_{82}$ are astonishingly similar to those of $Sc_2C_2@C_{82}$-III reported by Iiduka et al.[33] (see Supporting Information S6 for further details). For the latter, the authors observed an irreversible first reduction at −0.94 V, two reversible reductions at −1.15 and −1.60 V, and one reversible oxidation at 0.47 V vs $Fc^{+/0}$ in *o*-DCB solution. Such a close similarity in the redox properties of $Sc_2S@C_{82}$ and $Sc_2C_2@C_{82}$-III indicates that these clusterfullerenes have the same carbon cage, C_{82}-C_{3v}(8).

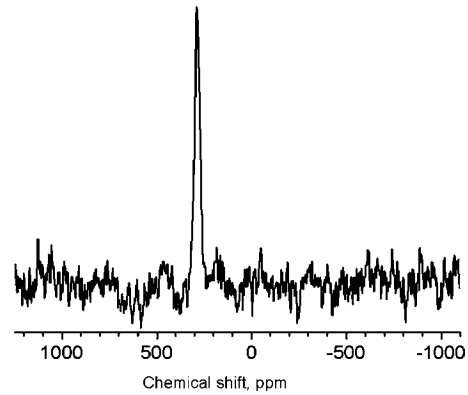

Figure 5. ^{45}Sc NMR spectrum of $Sc_2S@C_{82}$.

The above conclusion on the similarity of the electronic state of the carbon cage of $Sc_2S@C_{82}$ with $Sc_2C_2@C_{82}$ is also supported by the FTIR spectroscopic study. The FTIR spectrum of the $Sc_2S@C_{82}$ shown in Figure 4 exhibits a pronounced similarity to the FTIR spectrum of the $Sc_2C_2@C_{82}$-C_{3v}(8),[34] especially in the range of the tangential vibrations of the carbon cage (1100−1700 cm^{-1}). This is a further argument in favor of the C_{82}-C_{3v}(8) cage isomer for $Sc_2S@C_{82}$ (see below for more detailed discussion of the spectrum in comparison to the results of DFT calculations).

ESR spectroscopic study shows that the $Sc_2S@C_{82}$ is ESR silent. Only a single line at 290 ppm was found in the ^{45}Sc NMR spectrum of $Sc_2S@C_{82}$ (Figure 5), showing that either two Sc atoms are equivalent, or the cluster rotates at such rates that the signal of different Sc atoms are averaged. Note that the ^{45}Sc NMR spectrum of the major isomer of $Sc_2C_2@C_{82}$-III has also exhibited a single line at ca. 225 ppm in the broad temperature range.[35]

Elucidation of the Molecular Structure of $Sc_2S@C_{82}$. The trends in stability of the cage isomers of endohedral metallofullerenes can be rationalized by a formal transfer of the appropriate number of electrons from the encapsulated species to the carbon

(31) Inakuma, M.; Yamamoto, E.; Kai, T.; Wang, C. R.; Tomiyama, T.; Shinohara, H.; Dennis, T. J. S.; Hulman, M.; Krause, M.; Kuzmany, H. *J. Phys. Chem. B* **2000**, *104* (21), 5072–5077.
(32) Inakuma, M.; Shinohara, H. *J. Phys. Chem. B* **2000**, *104* (32), 7595–7599.
(33) Iiduka, Y.; Wakahara, T.; Nakajima, K.; Nakahodo, T.; Tsuchiya, T.; Maeda, Y.; Akasaka, T.; Yoza, K.; Liu, M. T. H.; Mizorogi, N.; Nagase, S. *Angew. Chem., Int. Ed.* **2007**, *46* (29), 5562–5564.
(34) Krause, M.; Hulman, M.; Kuzmany, H.; Dennis, T. J. S.; Inakuma, M.; Shinohara, H. *J. Chem. Phys.* **1999**, *111* (17), 7976–7984.

cage. For instance, a formal 6-fold electron transfer can be ascribed to the nitride clusterfullerenes $(M^{3+})_3N^{3-}@C_{2n}{}^{6-}$,[30,36−38] and we have recently shown that the cage isomers of $M_3N@C_{2n}$ clusterfullerenes can be reliably predicted on the basis of the broad search of the lowest energy $C_{2n}{}^{6-}$ isomers followed by computations of the limited number of the $M_3N@C_{2n}$ isomers.[30] By this method, we have elucidated molecular structures of $Sc_3N@C_{70}$-C_{2v}(8054),[39] $Sc_2DyN@C_{76}$-C_s(17490),[40] and $M_3N@C_{78}$-C_2(22010)[41] (M = Dy, Tm; recently, an X-ray single structure with M = Gd was published[42]) and proposed two low energy isomers of $M_3N@C_{82}$,[30] C_{2v}(39705) and C_s(39663), the latter being recently confirmed by X-ray single-crystal study of $Gd_3N@C_{82}$.[27] For other cage sizes this method also leads to the experimentally available isomers of $M_3N@C_{2n}$.[30] On the basis of the analogy to the $M_3N@C_{2n}$ species as well as on the results of spectroscopic studies discussed above, a 4-fold electron transfer from the M_2S cluster to the C_{82} can be proposed, i.e., $(M^{3+})_2S^{2-}@C_{82}{}^{4-}$. In this way, the sulfide cluster is analogous to the carbide cluster, in which the 4-fold cluster-to-cage electron transfer is proposed.[18,43] Relative stabilities of the IPR isomers of C_{82} in the charge states have been studied by several groups,[6,43,44] all agreeing that the lowest energy IPR isomer of $C_{82}{}^{4-}$ is C_{3v}(8), and this structure is indeed proved by NMR and single-crystal X-ray diffractions studies for the main isomers of $Sc_2C_2@C_{82}$[19,33,45] and $Y_2C_2@C_{82}$.[22,46,47] Importantly, this isomer also has the highest HOMO−LUMO gap in the 4− state.[43] In addition to the well-studied IPR isomers of C_{82}, in this work we have also considered the non-IPR isomers of C_{82} and found that the lowest energy non-IPR isomer of $C_{82}{}^{4-}$, C_{2v}(39705), is the fourth in the list of the most stable isomers at the PBE/TZ2P level, being 82 kJ/mol higher in energy than the IPR C_{3v}(8) isomer (see Table 1 and Supporting Information S7 for the list of the most stable isomers with their relative energies and HOMO−LUMO gaps). Two other stable isomers, C_{2v}(9) and C_s(6), are 12 and 35 kJ/mol higher in energy than the C_{3v}(8) isomer, and these structures are known for the minor isomers of $M_2C_2@C_{82}$.[22,31,48] Thus, one may expect that the major isomer of $M_2S@C_{82}$ sulfide clusterfullerenes is also based on the C_{3v}(8) cage. To prove this suggestion we have performed DFT calculations of the four cage isomers of $Sc_2S@C_{82}$ based on the four lowest energy $C_{82}{}^{4-}$ isomers (for each cage isomer, several conformations of the cluster inside the cage were considered). Calculations have shown that the lowest energy conformer of $Sc_2S@C_{82}$-C_{3v}(8) is indeed the most stable structure. Relative energy of the $Sc_2S@C_{82}$-C_s(6) isomer is only 1.6 kJ/mol; however, this isomer has a considerably smaller HOMO−LUMO gap (0.86 eV vs 1.20 eV in C_{3v}(8) isomer). Importantly, the encapsulation of the sulfide cluster considerably increases the HOMO−LUMO gaps compared to the $C_{82}{}^{4-}$.

Table 1. Relative Energies and HOMO-LUMO Gaps of the Four Most Stable Isomers of $C_{82}{}^{4-}$ and the Corresponding Isomers of $Sc_2S@C_{82}$[a]

	$C_{82}{}^{4-}$		$Sc_2S@C_{82}$	
cage isomer[b]	*E*, kJ/mol	gap, eV	*E*, kJ/mol	gap, eV
39717 C_{3v}-(8)	**0.0**	**0.93**	**0.0**	**1.20**
39718 C_{2v}-(9)	12.1	0.37	19.7	0.75
39715 C_s-(6)	34.9	0.45	1.6	0.86
39705 C_{2v}	82.1	0.51	119.1	0.20

[a] DFT calculations at the PBE/TZ2P level. [b] Numbers of the cage isomers are given in accordance to the Folwer−Manolopoulos[49] spiral algorithm; the more common numbers of the IPR isomers are also listed in parentheses.

In summary, DFT calculations show that on the basis of its low energy and large HOMO−LUMO gap, the C_{82}-C_{3v}(8) is the most probable cage structure of the isolated $Sc_2S@C_{82}$ sulfide clusterfullerene. This proposed cage isomeric structure is also strongly supported by the experimental results in UV−vis−NIR and FTIR spectroscopic analysis and electrochemical study as discussed above.

Analysis of the FTIR Vibrational Spectrum. High structural sensitivity of the vibrational spectroscopy makes this method a valuable tool for the structure determination of endohedral fullerenes. Earlier we have used FTIR spectroscopy to elucidate molecular structures of different endohedral fullerenes like $Sc_3N@C_{70}$,[39] $DySc_2N@C_{76}$,[40] $M_3N@C_{78}$ (M = Dy, Tm),[41] and $TiSc_2N@C_{80}$.[50] Figure 4 also compares FTIR spectrum of $Sc_2S@C_{82}$ to the DFT-computed spectrum of the lowest energy conformer of $Sc_2S@C_{82}$. Although an exact correspondence of the experimental and the computed spectra of $Sc_2S@C_{82}$ can hardly be expected because of the fast rotation of the cluster (see below), the main vibrational features of the carbon cage are reliably reproduced by the calculations. At the same, DFT-computed spectra of other cage isomers of $Sc_2S@C_{82}$ do not match the experimental spectrum (see Figure S9 in Supporting Information).

Special attention in the analysis of the IR spectra was devoted to the metal−sulfur vibrations. It was shown earlier that in the nitride clusterfullerenes, the antisymmetric metal−nitrogen stretching mode has high IR intensity and is usually observed in the 500−700 cm^{-1} range (in particular, at 597 cm^{-1} for $Sc_3N@C_{80}$[51]). It makes this vibration a convenient marker of the cluster state and structure, as we have shown in a series of studies on nitride clusterfullerenes.[6,39−41,50,52−58] For the sulfide

(35) Miyake, Y.; Suzuki, S.; Kojima, Y.; Kikuchi, K.; Kobayashi, K.; Nagase, S.; Kainosho, M.; Achiba, Y.; Maniwa, Y.; Fisher, K. *J. Phys. Chem.* **1996**, *100*, 9579–9581.
(36) Chaur, M. N.; Valencia, R.; Rodriguez-Fortea, A.; Poblet, J. M.; Echegoyen, L. *Angew. Chem., Int. Ed.* **2009**, *48* (8), 1425–1428.
(37) Campanera, J. M.; Bo, C.; Poblet, J. M. *Angew. Chem., Int. Ed.* **2005**, *44* (44), 7230–7233.
(38) Campanera, J. M.; Bo, C.; Olmstead, M. M.; Balch, A. L.; Poblet, J. M. *J. Phys. Chem. A* **2002**, *106* (51), 12356–12364.
(39) Yang, S. F.; Popov, A. A.; Dunsch, L. *Angew. Chem., Int. Ed.* **2007**, *46* (8), 1256–1259.
(40) Yang, S.; Popov, A. A.; Dunsch, L. *J. Phys. Chem. B* **2007**, *111* (49), 13659–13663.
(41) Popov, A. A.; Krause, M.; Yang, S. F.; Wong, J.; Dunsch, L. *J. Phys. Chem. B* **2007**, *111* (13), 3363–3369.
(42) Beavers, C. M.; Chaur, M. N.; Olmstead, M. M.; Echegoyen, L.; Balch, A. L. *J. Am. Chem. Soc.* **2009**, *131* (32), 11519–11524.
(43) Valencia, R.; Rodríguez-Fortea, A.; Poblet, J. M. *J. Phys. Chem. A* **2008**, *112* (20), 4550–4555.
(44) Kobayashi, K.; Nagase, S. *Chem. Phys. Lett.* **1998**, *282* (3−4), 325–329.
(45) Yamazaki, Y.; Nakajima, K.; Wakahara, T.; Tsuchiya, T.; Ishitsuka, M. O.; Maeda, Y.; Akasaka, T.; Waelchli, M.; Mizorogi, N.; Nagase, H. *Angew. Chem., Int. Ed.* **2008**, *47*, 7905–7908.
(46) Nishibori, E.; Ishihara, M.; Takata, M.; Sakata, M.; Ito, Y.; Inoue, T.; Shinohara, H. *Chem. Phys. Lett.* **2006**, *433* (1−3), 120–124.
(47) Nishibori, E.; Narioka, S.; Takata, M.; Sakata, M.; Inoue, T.; Shinohara, H. *ChemPhysChem* **2006**, *7* (2), 345–348.
(48) Ito, Y.; Okazaki, T.; Okubo, S.; Akachi, M.; Ohno, Y.; Mizutani, T.; Nakamura, T.; Kitaura, R.; Sugai, T.; Shinohara, H. *ACS Nano* **2007**, *1* (5), 456–462.
(49) Fowler, P.; Manolopoulos, D. E. *An Atlas of Fullerenes*; Clarendon Press: Oxford, U.K., 1995.
(50) Yang, S.; Chen, C.; Popov, A.; Zhang, W.; Liu, F.; Dunsch, L. *Chem. Commun.* **2009**, 6391–6393.
(51) Krause, M.; Kuzmany, H.; Georgi, P.; Dunsch, L.; Vietze, K.; Seifert, G. *J. Chem. Phys.* **2001**, *115* (14), 6596–6605.

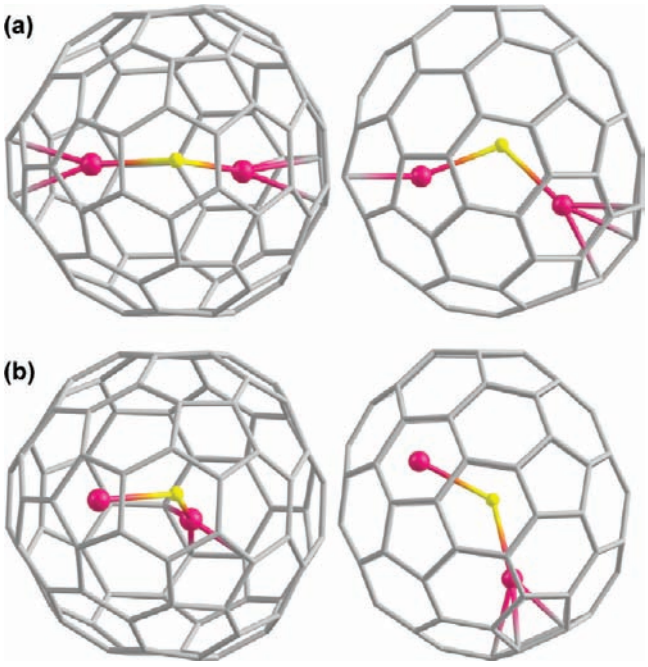

Figure 6. (a) Molecular structure of the lowest energy conformer of $Sc_2S@C_{82}$-C_{3v}(8) in two projections of the carbon cage (left, C_3 axis is perpendicular to the paper; right, C_3 axis is perpendicular to symmetry plane); carbon cage is gray, Sc atoms are magenta, sulfur atom is yellow. (b) The same for the high energy conformer (ΔE = 55 kJ/mol, gap =0.63 eV). According to Hessian computations, both structures are true energy minima (see Supporting Information S8 for more details).

clusterfullerenes, our computations have shown that the corresponding metal−sulfur vibration is significantly red-shifted to 382 cm^{-1} because of the larger atomic mass of sulfur. Indeed, when the spectral range was expanded to the far-IR, a strong absorption at 383 cm^{-1} was found.

Dynamics of the Metal Sulfide Cluster. Detailed calculations have shown that the Sc_2S cluster can adopt several almost isoenergetic positions inside the C_{82}-C_{3v}(8) cage (referred to as conformers hereafter). In particular, four conformers were found within the energy range of only 2 kJ/mol and the HOMO−LUMO gaps of 1.16−1.20 eV. In these structures, the Sc_2S cluster is bent with the Sc−S−Sc angle of ca. 110° (114° in the lowest energy conformer) and the Sc−S bondlengths in the range of 2.35−2.37 Å (2.363 and 2.367 Å in the lowest energy conformer, Figure 6a). All these conformers are related to each other by the rotation of the cluster around the C_3 axis of the cage, the sulfur atom being located on this axis and the cluster plane being nearly parallel to the axis. At the same time, we have also found that two conformers which have considerably different orientations of the cluster (so that they cannot be obtained from the lowest energy conformer by simple rotation around the C_3-axis) are much higher in energy (26 and 55 kJ/mol; see Figure 6b for the higher energy structure) and have smaller HOMO−LUMO gaps (1.02 and 0.63 eV, respectively). These results show that the cluster rotates freely around the C_3 axis of the cage. The Sc atoms are hence equivalent on the NMR time scale, which explains the single line ^{45}Sc NMR spectrum measured experimentally for $Sc_2S@C_{82}$. At the same time, declination of the cluster plane from the C_3 axis of the cage is considerably hindered.

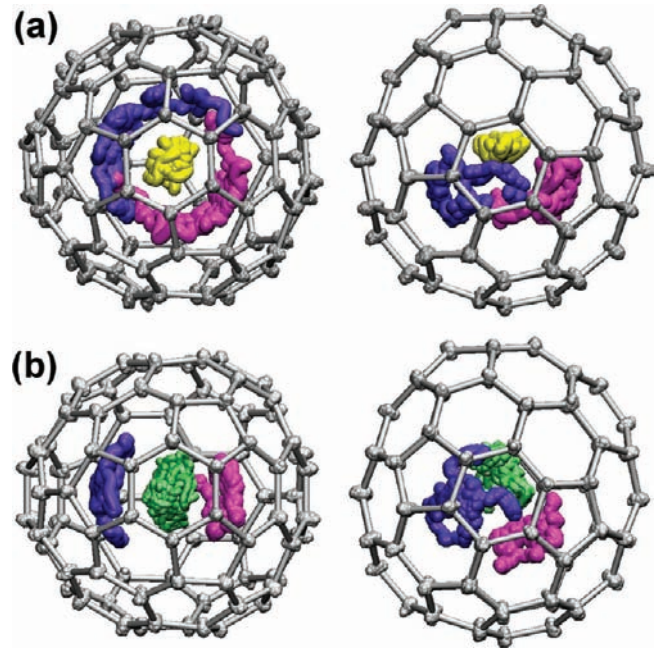

Figure 7. (a) BOMD trajectory of $Sc_2S@C_{82}$ followed for 10 ps in the microcanonical ensemble after equilibration for 0.5 ps at 300 K; Sc atoms are blue and magenta, sulfur atom is yellow, carbon atoms are gray. (b) The same for $Sc_2C_2@C_{82}$; carbon atoms of the carbide unit are light green. For each molecule, two views are shown: one with the C_3 axis of the cage perpendicular to the paper, and the other one with the axis coplanar to the paper.

To get a deeper insight into the cluster dynamics, we have performed DFT Born−Oppenheimer molecular dynamics (BOMD) simulations. Figure 7 shows the trajectory of the $Sc_2S@C_{82}$ followed for 10 ps in the microcanonical ensemble after equilibration at 300 K for 0.5 ps. Results of the BOMD simulations are in perfect agreement with the dynamical scenario outlined above. The cluster exhibits rotation around the C_3 axis (more than the half-turn is accomplished over the 10 ps) with relatively small amplitude of declination.

Comparison of the Structure and Dynamics of $Sc_2S@C_{82}$ to Those of $Sc_2C_2@C_{82}$. The same cage isomer (C_{3v}(8)) suggests that the structure and the cluster dynamics of the sulfide, $Sc_2S@C_{82}$, can be similar to those of the carbide clusterfullerene, $Sc_2C_2@C_{82}$. Indeed, we have found that locations of the Sc atoms in the lowest energy conformer of $Sc_2S@C_{82}$ is very similar to that of the lowest energy conformer of $Sc_2C_2@C_{82}$ (however, in the carbide fullerene a C_s-symmetric structure is found, while the structure of $Sc_2S@C_{82}$ is slightly distorted from the C_s symmetry). Sc_2C_2 cluster is also bent (the angle between the two Sc−C_2 planes is 133°), the distance between the Sc atoms and the center of the C_2 unit is 2.177 Å (the smaller distance compared to the Sc−S bondlenghts is probably the reason of the larger bent angle). At the same time, calculations of the different conformers of $Sc_2C_2@C_{82}$ have shown that their relative energies are distributed in the somewhat larger range

(52) Krause, M.; Popov, A.; Dunsch, L. *ChemPhysChem* **2006**, *7* (8), 1734–1740.
(53) Yang, S. F.; Kalbac, M.; Popov, A.; Dunsch, L. *ChemPhysChem* **2006**, *7* (9), 1990–1995.
(54) Yang, S.; Popov, A. A.; Chen, C.; Dunsch, L. *J. Phys. Chem. C* **2009**, *113* (18), 7616–7623.
(55) Yang, S. F.; Popov, A. A.; Kalbac, M.; Dunsch, L. *Chem.—Eur. J.* **2008**, *14* (7), 2084–2092.
(56) Yang, S. F.; Popov, A. A.; Dunsch, L. *Chem. Commun.* **2008**, 2885–2887.
(57) Yang, S. F.; Troyanov, S. I.; Popov, A. A.; Krause, M.; Dunsch, L. *J. Am. Chem. Soc.* **2006**, *128* (51), 16733–16739.
(58) Yang, S. F.; Kalbac, M.; Popov, A.; Dunsch, L. *Chem.—Eur. J.* **2006**, *12* (30), 7856–7863.

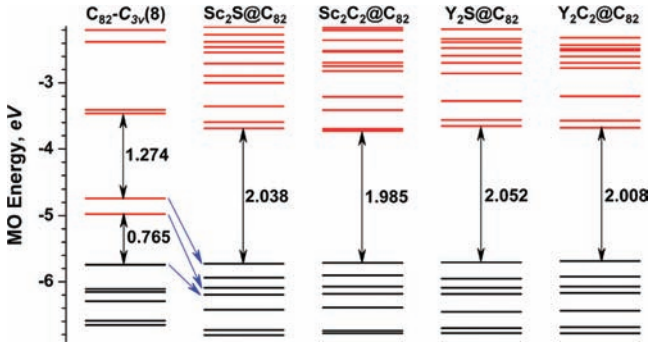

Figure 8. Kohn−Sham MO energy levels in C_{82}-C_{3v}(8) computed at the B3LYP/6-311G*//PBE/TZ2P level as compared to those of $Sc_2S@C_{82}$, $Sc_2C_2@C_{82}$, $Y_2S@C_{82}$, and $Y_2C_2@C_{82}$, all based on the C_{82}-C_{3v}(8) carbon cage. Occupied levels are shown in black, and unoccupied levels are shown in red.

(up to 20 kJ/mol; see refs 33, 43) than the energies of the most stable conformers of $Sc_2S@C_{82}$ found in this work. It shows that the rotation of the Sc_2C_2 cluster can be somewhat more hindered than the rotation of the Sc_2S cluster; at the same time, we could not find any specific preference of the rotation around the C_3 axis. BOMD simulations performed under the same conditions as for the $Sc_2S@C_{82}$ confirmed these conclusions. Displacements of the Sc atoms in $Sc_2C_2@C_{82}$ are not as pronounced as for the Sc atoms in the Sc_2S cluster on the 10 ps time scale, showing that rotation of the cluster is more hindered in the carbide clusterfullerene. At the same time, they are still rather large to give the free rotation on the NMR time scale.[19,35] Note also that the motions of the C_2 unit in the $Sc_2C_2@C_{82}$ are very complex and they definitively cannot be described as the in-plane rotation, as found in another carbide clusterfullerene, $Sc_2C_2@C_{84}$.[59,60] For this reason, the quantized rotation of the C_2 unit, discovered by Krause et al. for the $Sc_2C_2@C_{84}$,[59] was not to be observed in $Sc_2C_2@C_{82}$.[31,61] Note that the recent BOMD study of $Sc_3C_2@C_{80}$ has also shown complex motion of the carbide unit.[62]

Electronic Structure of $M_2S@C_{82}$ and $M_2C_2@C_{82}$. Figure 8 shows Kohn−Sham MO levels in the empty C_{82} cage as well as in $Sc_2S@C_{82}$, $Sc_2C_2@C_{82}$, and their yttrium analogues, $Y_2S@C_{82}$ and $Y_2C_2@C_{82}$, computed at the B3LYP//PBE level. First of all, it can be clearly seen that the energies of the frontier orbitals in sulfide and carbide clusterfullerenes are very similar (in perfect agreement with results of the cyclic voltammetry study) and that the formal 4-fold electron transfer from the sulfide cluster to the carbon cage is indeed confirmed by the MO analysis. Importantly, the electron transfer to the two lowest vacant orbitals of the C_{82}-C_{3v}(8) results in their strong stabilization, while the energy of the LUMO+2 of the empty cage remains almost unchanged in the clusterfullerenes. As a result, HOMO−LUMO gaps in the clusterfullerenes are considerably increased as compared to the (LUMO+2)−(LUMO+3) gap in the empty cage, as we have noted above.

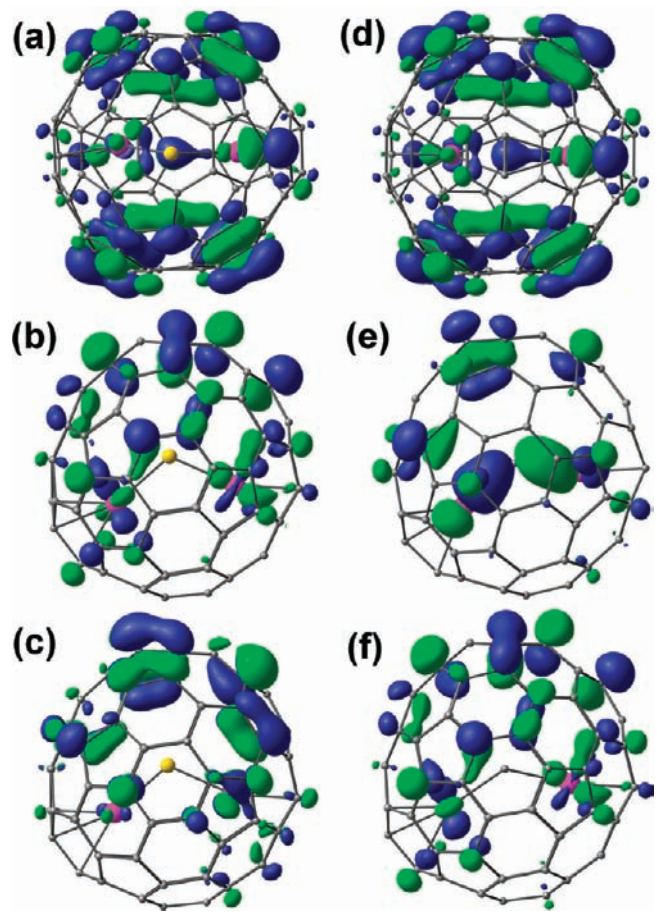

Figure 9. HOMO (a), LUMO (b), and LUMO+1 (c) of $Sc_2S@C_{82}$ compared to HOMO (d), LUMO (e) and LUMO+1 (f) of $Sc_2C_2@C_{82}$.

The frontier occupied orbitals are predominantly localized on the carbon cage (Figure 9), and hence it is not surprising that their energies and shapes are very similar in all four clusterfullerenes. The differences are more enhanced for the virtual orbitals. In $Sc_2S@C_{82}$, the two lowest unoccupied orbitals are also cage orbitals, while a set of scandium-localized orbitals follows at higher energy. In $Sc_2C_2@C_{82}$, LUMO is localized on the cluster, while LUMO+1 is the cage orbital very similar to the LUMO of $Sc_2S@C_{82}$ (note that our recent calculations of the anion of $Sc_2C_2@C_{82}$ have shown that the cage orbital is stabilized in the charged state, and SOMO corresponds to the LUMO+1 of the neutral form[63]). For this reason, the HOMO−LUMO gap of $Sc_2C_2@C_{82}$ is slightly smaller than that of $Sc_2S@C_{82}$. In the case of Y-based structures, both LUMO and LUMO+1 are cage orbitals like those in $Sc_2S@C_{82}$ since Y-based orbitals are higher in energy (similar situation was found in $Sc_3N@C_{80}$ and $Y_3N@C_{80}$: while the LUMO of $Sc_3N@C_{80}$ is mainly localized on the cluster, the cluster contribution to the LUMO of $Y_3N@C_{80}$ is very small[63,64]).

Further details of the bonding in sulfide clusterfullerenes were obtained using topological analysis of the electron density (in the framework of the quantum theory of atoms-in-molecule,[65]

(59) Krause, M.; Hulman, M.; Kuzmany, H.; Dubay, O.; Kresse, G.; Vietze, K.; Seifert, G.; Wang, C.; Shinohara, H. *Phys. Rev. Lett.* **2004**, *93* (13), 137403.
(60) Michel, K. H.; Verberck, B.; Hulman, M.; Kuzmany, H.; Krause, M. *J. Chem. Phys.* **2007**, *126* (6), 064304.
(61) Krause, M.; Popov, V. N.; Inakuma, M.; Tagmatarchis, N.; Shinohara, H.; Georgi, P.; Dunsch, L.; Kuzmany, H. *J. Chem. Phys.* **2004**, *120* (4), 1873–1880.
(62) Taubert, S.; Straka, M.; Pennanen, T. O.; Sundholm, D.; Vaara, J. *Phys. Chem. Chem. Phys.* **2008**, *10*, 7158–7168.
(63) Popov, A. A.; Dunsch, L. *J. Am. Chem. Soc.* **2008**, *130* (52), 17726–17742.
(64) Valencia, R.; Rodriguez-Fortea, A.; Clotet, A.; de Graaf, C.; Chaur, M. N.; Echegoyen, L.; Poblet, J. M. *Chem.—Eur. J.* **2009**, *15* (41), 10997–11009.
(65) Bader, R. F. W. *Atoms in Molecules—A Quantum Theory*; Oxford University Press: Oxford, 1990.

Table 2. MO Energies (eV), Bader Charges (q), Delocalization Indices (δ), and Normalized Total Energy Density at Bond Critical Points (H_{bcp}/ρ_{bcp}) in $M_2S@C_{82}$ and $M_2C_2@C_{82}$ (M = Sc, Y)[a]

	HOMO, eV	LUMO, eV	gap, eV	q(M)	q(S/C_2)	q(C_{82})	δ(M, S/C_2)	δ(M, C_{82})	$-H_{bcp}/\rho_{bcp}$, au
$Sc_2S@C_{82}$	−5.725	−3.687	2.038	1.69	−1.18	−2.19	0.704	1.942	0.251
$Sc_2C_2@C_{82}$	−5.714	−3.729	1.985	1.76	−1.38	−2.09	0.635	1.944	0.146
$Y_2S@C_{82}$	−5.706	−3.655	2.052	1.83	−1.20	−2.46	0.710	1.885	0.221
$Y_2C_2@C_{82}$	−5.687	−3.679	2.008	1.89	−1.38	−2.40	0.640	1.897	0.126

[a] DFT calculations at the B3LYP//PBE level. Because two metal atoms in $M_2S@C_{82}$ and $M_2C_2@C_{82}$ exhibit very similar topological parameters, only the averaged value is shown for each molecule.

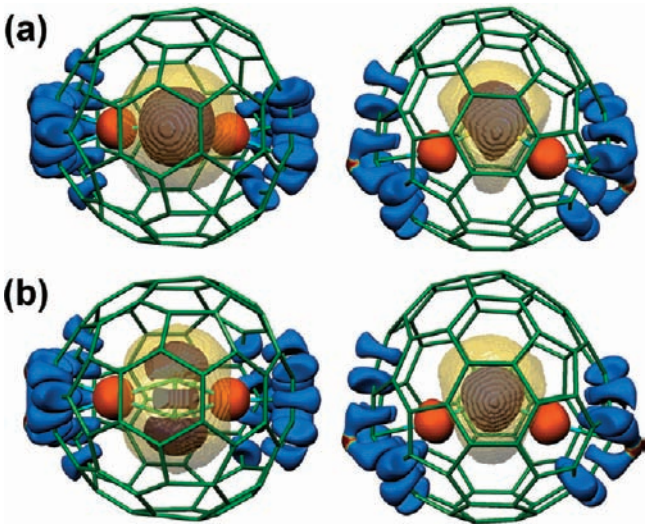

Figure 10. Electron localization function (η = 0.72 isosurface) in (a) $Sc_2S@C_{82}$ and (b) $Sc_2C_2@C_{82}$; two orientations are shown for each molecule. Light blue = V(Sc,C,C) basins, orange = Sc core basins, red = monosynaptic V(C) basins, dark blue = trisynaptic valence V(S, Sc, Sc) or V(Sc, C, C) intracluster basins. Bader volumes of the sulfur atom and the carbide unit are shown as yellow transparent surfaces.

QTAIM) and the electron localization function[66−68] (ELF). Table 2 lists Bader charges of the metal and sulfur atoms and carbide units. Here the charges of the metal atoms are very similar in all four clusterfullerenes, the charges in the carbide clusterfullerenes being slightly larger than in sulfide clusterfullerenes, and the charges of the yttrium atoms being ca. 0.15 e larger than those of the scandium atoms. The sulfur bears a considerable negative charge (ca. −1.20 e), which is however somewhat smaller than the charge of the carbide unit (−1.38 e). The Bader volumes of the sulfur atom and the carbide units are also very similar (see Figure 10). The total charge on the carbon cage exceeds −2.0 e for all four clusterfullerenes but is smaller than −2.5 e. Important information abut the bonding can be obtained by the analysis of the delocalization indices, δ(A, B), which are defined as the number of the electron pairs shared between the atoms A and B (in other words, delocalization indices can be understood as "bond orders").[69,70] The δ(Sc, S) and δ(Y, S) values are close to 0.7, approaching the value expected for the ordinary covalent bond. The covalency of the metal−sulfur bonding is also confirmed by the negative values of the total energy density at the metal−sulfur bond critical points (H_{bcp}, see Table 2 for the values of H_{bcp} normalized to the values of electron density at bond critical points, ρ_{bcp}). Note that δ(Sc, C_2) and δ(Y, C_2) as well as the H_{bcp}/ρ_{bcp} values for the metal-carbide bonds are smaller than their sulfide counterparts, which points to the higher-degree of covalent interactions in sulfide clusters compared to the corresponding carbide. Finally, note that each metal atom shares ca. 1.9 electron pairs with the carbon cage (see δ(M, C_{82}) values in Table 2). The fact that these electron pairs are not completely transferred to the carbon cages (as can be seen from the smaller charges of the cages) shows that there is also considerable covalency in the metal−cage interactions as pointed in our recent study.[70]

A very illustrative visualization of the metal−cage bonding can be obtained using the ELF isosurfaces as shown in Figure 10. While in the empty fullerene molecule only disynaptic valence carbon−carbon basins, V(C, C), are found, formation of the metal−cage bond is seen in ELF as an extension of some V(C,C) basins in the vicinity of the metal atoms (see also analogous observation in ref 62) and their transformation into the trisynaptic V(M, C, C) basins. These basins are shown in light blue in Figure 10 (for clarity, V(C,C) basins and carbon core basins are not shown). In some cases, we have also found a formation of the monosynaptic valence carbon basins, V(C), for the cage atoms experiencing the strongest interaction with the metal atoms (in most cases, metal−cage bond path is found for these carbon atoms). Note that valence monosynaptic basins are usually associated with lone electron pairs (however, in the case of $Sc_2S@C_{82}$ and $Sc_2C_2@C_{82}$ their occupations are ca. 0.2 e). Two facts should be pointed out. First, the number of the V(Sc, C, C) basins is rather large for each Sc atom, showing that the metal atoms are bonded to the electron density of the large fragment of the cage; however, these are not *completely* delocalized interactions. Second, the number and the spatial distribution of the V(Sc, C, C) basins in $Sc_2S@C_{82}$ and $Sc_2C_2@C_{82}$ are very similar, which confirms the similarity of the cluster−cage interactions in sulfide and carbide clusterfullerenes.

Conclusions

In summary, we have shown for the first time that a new endohedral sulfide clusterfullerene $M_2S@C_{82}$ (M = Sc, Y, Dy, and Lu) has been successfully synthesized using a new synthetic route in applying the new solid source containing sulfur along with nitrogen in a limited amount in the graphite rods for the arc-burning process. While for trimetallic nitride clusters the fullerene cage is predominantly C_{80}-I_h, in the case of sulfur the C_{82} cage is the dominating fullerene structure. The cage isomeric structure of $M_2S@C_{82}$ (M = Sc, Y, Dy, and Lu) was determined to be $C_{3v}(8)$ thus pointing to the fact that, despite of the situation in nitride cluster with non-IPR C_{82} cages within $Gd_3N@C_{82}$, the new sulfide cluster $M_2S@C_{82}$ prefers an IPR cage (C_{82}-$C_{3v}(8)$). This is due to the fact that the formal transfer of four electrons from the cluster to the cage results in the most

(66) Silvi, B.; Savin, A. *Nature* **1994**, *371*, 683–686.
(67) Savin, A.; Nesper, R.; Wenger, S.; Fassler, T. F. *Angew. Chem., Int. Ed.* **1997**, *36*, 1808–1832.
(68) Kohout, M.; Wagner, F. R.; Grin, Y. *Theor. Chem. Acc.* **2002**, *108* (3), 150–156.
(69) Matito, E.; Sola, M. *Coord. Chem. Rev.* **2009**, *253* (5−6), 647–665.
(70) Popov, A. A.; Dunsch, L. *Chem.−Eur. J.* **2009**, *15* (38), 9707–9729.

stable $C_{3v}(8)$ cage isomer for the charged state as the same to that in carbide clusterfullerenes, $M_2C_2@C_{82}$. The further analysis of the electronic structure shows that the bonding in sulfide and carbide clusterfullerenes is very similar, the sulfur atom resembling the carbide unit. At the same time, the metal−sulfur interactions exhibit a higher degree of covalency than that of the metal−carbide bonding, as can be shown by the slightly smaller charges of the metal atoms in sulfide clusters and smaller negative charge of sulfur in M_2S cluster compared to the charge of the carbide unit on M_2C_2 clusters. With the successful synthesis and isolation of several new representative sulfide clusterfullerenes, this study opens up a new route to the novel endohedral fullerenes.

Experimental Section

The new synthetic route to sulfide cluster fullerenes $M_2S@C_{82}$ is based on the Krätschmer−Huffman arc burning method. For the synthesis of sulfide cluster fullerenes, the solid sulfur source guanidium thiocyanate (CH_5N_3HSCN, in abbreviation GT) was added to the metal/graphite powder mixture using an optimized molar ratio of GT/metal/C = 2.5:1:10, metal M = Sc, Y, Dy, and Lu). The DC-arc discharging was carried out under 200 mbar He and current of 100 A. After DC-arc discharging, the soot was collected under ambient condition and was first pre-extracted with acetone for several hours to remove nonfullerene hydrocarbon byproduct and other low molecular structures. Subsequently the mixture was Soxhlet extracted by CS_2 for 20 h. The resulting brown-yellow solution was distilled to remove CS_2, immediately redissolved in toluene, and subsequently passed through a 0.2 μm Telflon filter (Sartorius AG, Germany) for HPLC separation. The separation of $M_2S@C_{82}$ clusterfullerene was performed by multistep HPLC as follow. In the first-step HPLC running in a linear combination of two analytical 4.6 mm × 250 mm Buckyprep columns (Nacalai Tesque, Japan), fraction **A** with retention time between 37.5 and 40.9 min was collected (see Figure 1a) and was then subject to the second-step HPLC isolation by recycling HPLC running in a 10 mm × 250 mm Buckyprep-M column (Nacalai Tesque, Japan). Consequently the successful isolation of fractions **A-1** by removal of fraction **A-2** was achieved.

The mass spectrometric characterization was done by MALDI-TOF mass spectrometry using the Biflex III spectrometer (Bruker, Germany), and the positive and negative ions of the fullerenes were detected. UV−vis−NIR spectra of the purified fullerene samples were preferably measured in toluene solution using an UV 3101 PC spectrometer (Shimadzu, Japan) using a quartz cell of 1 mm layer thickness and 1 nm resolution. For FTIR spectroscopic measurements solutions of the endohedral fullerene in toluene were drop-casted onto KBr single crystal disks. The residing toluene solvent was removed by heating the polycrystalline films in a vacuum of 10^{-6} mbar at 250 °C for 3 h. FTIR spectra were recorded at room temperature by an IFS 66v spectrometer (Bruker, Germany). The ^{45}Sc NMR spectroscopic study was performed at 121.5 MHz in a multiprobe head PH 1152Z of an Avance 500 spectrometer (Bruker) at room temperature in carbon disulfide solutions with d_6-acetone as a lock and a 0.2 M $Sc(NO_3)_3$ solution in concentrated HNO_3 as a reference. Electron spectroscopy for chemical analysis (ESCA) was performed using a PHI 5600 CI (Physical Electronics) analyzer with the following standard parameters: Al−Kα X-rays, monochromatized, 350 W. A platinum sheet with dimensions of 10 mm ×10 mm was used as substrate for fullerene deposition.

Details of Computations. Optimization of the molecular structure of all species reported in this work was performed using PBE functional[71] and TZ2P-quality basis set (full-electron {6,3,2}/(11s,6p,2d) for C atoms, {10,6,2}/{15s,11p,2d} for S atoms, and SBK-type effective core potential for Sc and Y atoms with {5,5,4}/(9s,9p,8d) valence part) implemented in the PRIRODA package.[72,73] This basis set is abbreviated in the manuscript as TZ2P. The code employed expansion of the electron density in an auxiliary basis set to accelerate evaluation of the Coulomb and exchange-correlation terms.[72]

For the topological analysis, the electron density of EMFs was calculated at the B3LYP level with the use of Firefly/PC GAMESS package[74] and 6-311G* basis set for C, S, and Sc atoms and full-electron TZVP {8,6,5}/(19s,14p,9d) basis set for Y atoms.[75] QTAIM (quantum theory of atoms in molecules) analysis of the electron densities was performed with the use of AIMAll code (Version 08.05.04, http://aim.tkgristmill.com). The PROMEGA algorithm was used for the integration, since less time-demanding PROAIM algorithm often failed, especially for the metal atoms and the carbon atoms to which they are bonded. ELF analysis was performed using TopMoD 09 suite.[76]

Velocity Verlet algorithm with the time step 1.5 fs was used in Born−Oppenheimer molecular dynamics (BOMD) calculations. The energies and gradients were computed with PRIRODA using PBE functional, double-ζ quality {3,2}/(7s,4p) basis-set for cage carbon atoms and DZP-quality basis sets for sulfur, scandium and carbon atoms of the carbide unit (S {4,3,1}/(14s,11p,3d); Sc {6,5,3,1}/(19s,15p,11d,5f), and C {3,2,1}/(10s,7p,3d), respectively). Molecules were first equilibrated at 300 K for 0.6 ps by rescaling velocities when the deviation of the instant temperature from 300 K exceeded 20 K. Then, the trajectory was followed without thermostat (i.e., in microcanonical ensemble).

Visualization of the computational results was done using ChemCraft,[77] Molekel,[78] and VMD.[79]

Acknowledgment. We cordially acknowledge the technical assistance of K. Leger, S. Schiemenz, and F. Ziegs (all at IFW Dresden). S.Y. thanks the National Natural Science Foundation of China (nos. 20801052, 90921013), National Basic Research Program of China (No. 2010CB923300), and "100 Talents Programme of CAS" from Chinese Academy of Sciences for financial support. L.Z. appreciates financial support from Chinese Scholar Council. A.A.P. acknowledges AvH foundation for financial support and "SKIF-MSU" supercomputer at Moscow State University for computer time. Technical assistance of U. Nitzsche with local computer resources at IFW is highly appreciated.

Supporting Information Available: Determination of the optimized conditions for the synthesis of $Dy_2S@C_{82}$, isolation of $Sc_2S@C_{82}$ by recycling HPLC, estimation of the relative yield of $Sc_2S@C_{82}$ to those of $Sc_3N@C_{80}$ (I), XPS results, voltammetry of the fullerene structure, relative energies of C_{82}^{4-} isomers, conformers of $Sc_2S@C_{82}$-$C_{3v}(8)$, and comparison of computed IR spectra of different $Sc_2S@C_{82}$ isomers. This material is available free of charge via the Internet at http://pubs.acs.org.

JA909580J

(71) Perdew, J. P.; Burke, K.; Ernzerhof, M. *Phys. Rev. Lett.* **1996**, *77* (18), 3865–3868.
(72) Laikov, D. N. *Chem. Phys. Lett.* **1997**, *281*, 151–156.
(73) Laikov, D. N.; Ustynyuk, Y. A. *Russ. Chem. Bull., Int. Ed.* **2004**, *54* (3), 820–826.
(74) Granovsky, A. A. *PC GAMESS/Firefly, version 7.1.C*; http://classic-.chem.msu.su/gran/gamess/index.html, 2008.
(75) Ahlrichs, R.; May, K. *Phys. Chem. Chem. Phys.* **2000**, *2*, 943–945.
(76) Noury, S.; Krokidis, X.; Fuster, F.; Silvi, B. *Comput. Chem.* **1999**, *23*, 597–604.
(77) Zhurko, G. A. *ChemCraft, version 1.6*; http://www.chemcraftprog.com.
(78) Flukiger, P.; Luthi, H. P.; Portmann, S.; Weber, J. *Molekel 4.3*; Swiss Center for Scientific Computing: Manno, 2002; http://www.cscs.ch/molkel.
(79) Humphrey, W.; Dalke, A.; Schulten, K. *J. Mol. Graphics* **1996**, *14*, 33–38.